

1  
2  
3  
4  
5  
6  
7  
8  
9  
10  
11  
12  
13  
14  
15  
16  
17  
18  
19  
20  
21  
22  
23  
24  
25

Article type : Articles

**Running Header:** Multi-scale accretion-erosion analysis

**Title:** Environmental drivers of coral reef carbonate production and bioerosion: a multi-scale analysis

**Authors:** Nyssa J. Silbiger<sup>1,2\*</sup>, Megan J. Donahue<sup>1</sup>, and Russell E. Brainard<sup>3</sup>

**Affiliations:**

<sup>1</sup>University of Hawai‘i at Mānoa, Hawai‘i Institute of Marine Biology, P.O. Box 1346, Kāne‘ohe, HI, 96816

<sup>2</sup>California State University, Northridge, Department of Biology, 18111 Nordhoff Street Northridge, CA 91330-8303 (Current address)

<sup>3</sup>Coral Reef Ecosystem Program, Pacific Islands Fisheries Science Center, National Oceanographic and Atmospheric Administration, 1845 Wasp Blvd., Bldg. 176, Honolulu, HI 96818

**ABSTRACT**

The resilience of coral reefs depends on the balance between reef growth and reef breakdown, and their responses to changing environmental conditions. Across the 2500 km Hawaiian Archipelago, we quantified rates of carbonate production, bioerosion, and net accretion at regional, island, site, and within-site spatial scales and tested how carbonate production,

---

\* Nyssa.Silbiger@csun.edu

This is the author manuscript accepted for publication and has undergone full peer review but has not been through the copyediting, typesetting, pagination and proofreading process, which may lead to differences between this version and the [Version of Record](#). Please cite this article as [doi: 10.1002/ecy.1946](https://doi.org/10.1002/ecy.1946)

26 bioerosion, and net accretion rates respond to environmental conditions across different spatial  
27 scales. Overall, there were four major outcomes from this study: 1) bioerosion rates were  
28 generally higher in the populated Main Hawaiian Islands (MHI) than the remote, protected  
29 Northwestern Hawaiian Islands (NWHI), while carbonate production rates did not vary  
30 significantly between the two regions; 2) variability in carbonate production, bioerosion, and net  
31 accretion rates was greatest at the smallest within-reef spatial scale; 3) carbonate production and  
32 bioerosion rates were associated with distinct sets of environmental parameters; and 4) the  
33 strongest correlates of carbonate production, bioerosion, and net accretion rates were different  
34 between the MHI region and the NWHI region: in the MHI, the dominant correlates were %  
35 cover of macroalgae and herbivorous fish biomass for carbonate production and bioerosion,  
36 respectively, whereas in the NWHI, the top correlates were total alkalinity and benthic cover.  
37 This study highlights the need to understand accretion and erosion processes as well as local  
38 environmental conditions to predict net coral reef responses to future environmental changes.

39

40

41 **Keywords:** Spatial scale, coral reefs, net accretion, bioerosion, carbonate production, local  
42 variability, latitudinal gradients, pH, multiple stressors

### 43 **1. INTRODUCTION**

44 Worldwide, declines in coral cover and shifts in coral reef community composition have raised  
45 concerns about reef persistence and the shifting balance between reef accretion and net  
46 bioerosion (e.g., Gardner et al. 2003, Bruno and Selig 2007, Kennedy et al. 2013). Corals and  
47 other calcifiers (e.g. non-coral encrusting invertebrates and crustose coralline algae (CCA)) build  
48 reefs through the production of calcium carbonate ( $\text{CaCO}_3$ ) skeletons, while a diverse  
49 community of organisms bioerode reefs through grazing on (e.g., urchins, parrotfish) and boring  
50 into (e.g., boring sponges, sipunculids, and polychaetes)  $\text{CaCO}_3$  reef substrate (e.g., Hutchings  
51 2011, Tribollet and Golubic 2011). Anthropogenic stressors affect the accretion-erosion balance  
52 of coral reefs at a range of spatial scales from global ocean acidification (e.g., Hoegh-Guldberg  
53 et al. 2007, Silbiger and Donahue 2015) to regional overfishing (e.g., Brown-Saracino et al.  
54 2007, Kennedy et al. 2013) and local eutrophication (e.g., Fabricius 2005, Hutchings et al. 2005,

55 Le Grand and Fabricius 2011). These stressors threaten to shift reefs from a state of net accretion  
56 to net erosion. Experimental studies on bioerosion have increased in recent years, especially  
57 those focused on the impacts of rising temperature and ocean acidification on bioerosion rates  
58 (see, Tribollet et al. 2009, Wisshak et al. 2012, 2013, Enochs et al. 2015, Silbiger and Donahue  
59 2015). To predict how reefs may shift under future ocean conditions, experimental studies must  
60 be contextualized with measurements of *in-situ* accretion-erosion rates and across a range of  
61 environmental conditions. Three major factors influence accretion-erosion rates on coral reefs:  
62 the chemical environment, the physical environment, and biological interactions. Here, we  
63 address how each of these factors influences accretion-erosion rates across different spatial  
64 scales.

65 Shifts in environmental conditions can alter bioerosion rates through changes in the  
66 physiology and metabolic pathways of bioeroders. Seawater pH (and related carbonate  
67 parameters) and nutrients are the two groups of chemical drivers that have received the most  
68 attention on coral reefs. For example, both experimental (Tribollet et al. 2009, Wisshak et al.  
69 2012, Fang et al. 2013, Reyes-Nivia et al. 2013, Wisshak et al. 2013, Enochs et al. 2015, Silbiger  
70 and Donahue 2015) and correlative (Silbiger et al. 2014, DeCarlo et al. 2015, Enochs et al. 2016,  
71 Silbiger et al. 2016) studies have demonstrated that decreasing pH increases bioerosion. Many  
72 studies have also demonstrated that decreasing pH reduces calcification in corals and crustose  
73 coralline algae (e.g., Hoegh-Guldberg et al. 2007, Jokiel et al. 2008, Diaz-Pulido et al. 2012,  
74 Johnson and Carpenter 2012, Comeau et al. 2013). In several field studies, bioerosion increased  
75 in eutrophic relative to oligotrophic conditions (e.g., Le Grand and Fabricius 2011, DeCarlo et al.  
76 2015), likely due to increased food availability to filter feeding bioeroders. Field studies that  
77 examined the simultaneous impact of nutrients and ocean acidity on bioerosion have found  
78 different responses over different spatial scales (DeCarlo et al. 2015, Silbiger et al. 2016). In a  
79 within-reef study (~30m) (Silbiger et al. 2014, Silbiger et al. 2016), ocean acidity was the best  
80 predictor of reef bioerosion when compared to nutrients, chlorophyll, temperature, depth, and  
81 distance from shore. At a large-scale (~16,000 km) comparison across the Pacific Basin  
82 (DeCarlo et al. 2015), the positive relationship between bioerosion rates and ocean acidity was  
83 more pronounced at sites with higher nutrient concentrations.

84 Along with a changing chemical environment, physical parameters can affect the reef  
85 carbonate budget. For example, water movement can enhance growth of corals and other

86 calcifiers through transport and removal of nutrients and metabolic wastes (Hearn et al. 2001) or  
87 enhance erosion through dislodgement and abrasion (Madin and Connolly 2006). A study at  
88 Lizard Island, a relatively protected set of islands in the Great Barrier Reef approximately 5 km  
89 across, found that CCA and live coral cover was positively correlated with wave energy  
90 (Hamylton et al. 2013). Conversely, in a Pacific-wide study (~8000 km) that incorporated several  
91 exposed reef systems, coral cover declined with increasing wave energy (Williams et al. 2015).  
92 The chemical and physical environment can also interact as water residence times influence pH  
93 variability (Jury et al. 2013). These studies highlight the complex chemical and physical  
94 interactions influencing the accretion-erosion balance at different spatial scales.

95 Overlaid on a landscape of chemical and physical drivers, biological interactions also  
96 influence reef accretion-erosion rates. For example, grazers can influence bioerosion directly by  
97 incidentally removing  $\text{CaCO}_3$  substrate while grazing for algae (e.g., Bellwood 1995, Ong and  
98 Holland 2010) and can influence calcification indirectly by removing fleshy algae and relieving  
99 competitive interactions with CCA (Cebrian and Uriz 2006, Cebrian 2010, O'Leary and  
100 McClanahan 2010, González-Rivero et al. 2012). Benthic cover can also be a major factor  
101 affecting accretion-erosion rates. The amount of dead substrate on a reef is directly related to reef  
102 bioerosion rates, as bioeroders prefer dead substrate over live reef (Highsmith 1981b, Hutchings  
103 1986). Therefore, events that negatively impact live coral, such as large storms and bleaching  
104 events, can indirectly impact bioeroders.

105 While there have been several *in situ* studies focused on understanding controls on  
106 bioerosion rates and associated macroborer communities—chiefly at sites in Australia (e.g.,  
107 Davies and Hutchings 1983, Risk et al. 1995, Tribollet et al. 2002, Hutchings et al. 2005,  
108 Tribollet and Golubic 2005), the Caribbean (e.g., Neumann 1966, Rützler 1975, Perry et al.  
109 2012), and the Eastern Tropical Pacific (e.g., Scott and Risk 1988)—there have been no broad  
110 scale studies on accretion-erosion rates in the Hawaiian Archipelago; existing studies in Hawai'i  
111 have focused mainly on Kāne'ōhe Bay (White 1980, Tribollet et al. 2006, Silbiger et al. 2014,  
112 Silbiger et al. 2016). Here, we examine the patterns of carbonate production, bioerosion, and net  
113 accretion rates over multiple spatial scales at 29 sites across the Hawaiian Archipelago  
114 (~2500km). There were three goals for this study: 1) describe spatial patterns in rates of  
115 carbonate production (primarily from the settlement of crustose coralline algae), bioerosion, and  
116 net accretion on experimental blocks of dead coral substrate, 2) relate these patterns to chemical,

117 physical, and biological data from long-term monitoring and remote sensing data, and 3) test if  
118 the relationships between accretion-erosion rates and environmental drivers are consistent across  
119 spatial scales. We use a newly developed  $\mu$ CT methodology (Silbiger et al. 2014, Silbiger et al.  
120 2016) to measure *in situ* rates of carbonate production, bioerosion, and net accretion (calculated  
121 as percent change in volume) from experimental blocks of  $\text{CaCO}_3$  deployed across the Hawaiian  
122 Archipelago. In the first large scale application of this  $\mu$ CT method, we calculate carbonate  
123 production rates primarily from crustose coralline algae, and bioerosion rates from borers and  
124 grazers from an early successional community after a one-year deployment period.

## 125 **2. MATERIALS AND METHODS**

126 **2.1 Study Sites:** This study was conducted at 29 forereef sites (8-16 m depth) across six  
127 islands/atolls in the Hawaiian Archipelago (Fig. 1, S1, Table S1). Kure Atoll (KUR), Pearl and  
128 Hermes Atoll (PHR), Lisianski Atoll (LIS), and French Frigate Shoals (FFS) are atolls in the  
129 Northwestern Hawaiian Islands (NWHI) and protected by the Papahānaumokuākea Marine  
130 National Monument (PMNM), one of the largest and most remote marine protected areas in the  
131 world. O‘ahu and Maui are populated volcanic islands in the Main Hawaiian Islands (MHI).  
132 Twenty-seven of these sites were co-located with long-term monitoring sites maintained by the  
133 NOAA Coral Reef Ecosystem Program (CREP) to take advantage of pre-existing environmental  
134 data and research cruise logistics. The remaining two sites, O‘ahu-KBay and Maui-A27, were  
135 selected with similar depth and exposure characteristics. Maui-A27 was co-located with a long-  
136 term monitoring site maintained by the Hawai‘i Division of Aquatic Resources; O‘ahu-KBay is  
137 accessible from the Hawai‘i Institute of Marine Biology. The experimental design was explicitly  
138 hierarchical with  $n=5$  replicates per site, 4-5 sites per island/atoll, and 2 (MHI) or 4 (NWHI) sites  
139 per region.

140 **2.2 Carbonate Production, Bioerosion, and Net Accretion:** Five blocks (5 x 5 x 2.5 cm) cut  
141 from dead *Porites lobata* Dana 1846, collected above the high tide mark on O‘ahu, were  
142 deployed at each site for approximately one year (Fig. S2a, Table S1). Each block was carefully  
143 inspected and any block with obvious pre-existing boreholes was discarded. Blocks were then  
144 soaked in freshwater and autoclaved to sterilize the substrate. Two holes were drilled into each  
145 block for cable ties. At each site, one block was attached to each of five rebar stakes installed on  
146 the reef within a 5 m x 5 m area. Blocks were attached using cable ties and oriented vertically,  
147 such that the end of the block was in contact with the substrate (Fig. S2a). Because of the

148 remoteness of our field sites, all blocks were deployed and retrieved on NOAA ships with pre-  
149 determined cruise schedules. Blocks were deployed at FFS, LIS, and PHR sites in July/August  
150 2011 on NOAA cruise HA1103 and retrieved in August 2012 on NOAA cruise HA1204; at KUR  
151 sites in August 2012 on NOAA cruise HA1204 and retrieved in July 2013 on NOAA cruise  
152 SE1305; and at O‘ahu and Maui sites in September/October 2012 on NOAA cruise SE1207 and  
153 retrieved September/October 2013 with small boat operations (Table S1). While deploying  
154 blocks during different years is not ideal because recruitment of bioeroders can vary over time  
155 (e.g., Hutchings et al. 1992, Hutchings 2011), the remoteness of our sites and pre-determined  
156 cruise schedules and logistics made it unavoidable. All blocks were deployed on the reef for a  
157 full year and thus the substrate was available to bioeroders and calcifiers during all four seasons;  
158 all blocks were deployed between late July and early October. We recovered 143 of 145  
159 deployed experimental blocks; 122 blocks had before and after  $\mu$ CT scans of adequate quality  
160 for data analysis.

161 Carbonate production, bioerosion, and net accretion rates were calculated for each block  
162 by comparing before and after  $\mu$ CT scans of the entire blocks (Silbiger et al. 2014, Silbiger et al.  
163 2016).  $\mu$ CT is an X-ray technology that non-destructively images the external and internal  
164 structures of solid objects, resulting in a three-dimensional array of object densities. We used an  
165 eXplore CT120  $\mu$ CT (GE Healthcare Xradia, Inc) at the Cornell University Imaging Multiscale  
166 CT Facility to scan blocks before and after deployment (voltage = 100kV, current = 50mA). The  
167  $\mu$ CT was calibrated with a phantom (density standard) prior to running each batch of samples. A  
168 three-dimensional array of isotropic voxels at  $50 \mu\text{m}^3$  resolution was generated using the GE  
169 Console Software and the voxels were averaged to  $100 \mu\text{m}^3$  for data analysis. We used a  
170 threshold of 200 Hounsfield Units to separate coral from air (Silbiger et al. 2014). The number of  
171 voxels exceeding this threshold was multiplied by the voxel size ( $100 \mu\text{m}^3$ ) to give the total  
172 volume of  $\text{CaCO}_3$  for pre- and post-deployment blocks. The pre- and post-deployment scans  
173 were then aligned using an intensity-based registration technique from the MATLAB R2014b  
174 Image Processing Toolbox, converted to binary, and subtracted from one another resulting in a  
175 matrix of 0's, 1's, and -1's. All positive values were new pixels added to the post-deployment  
176 scan, which indicate carbonate production, negative values were pixels that were lost and  
177 indicate bioerosion, and zeros meant there was no change at that pixel between the two scans. All

178 values were summed and multiplied by the resolution of the scan to obtain the volume lost  
179 (bioerosion) or gained per block (carbonate production) (Fig. S2b,c).

180 Prior studies highlighted the need to analyze both carbonate production and bioerosion  
181 independently (Silbiger and Donahue 2015, Silbiger et al. 2016), but net accretion rates are also  
182 necessary for understanding long-term reef sustainability (Silbiger et al. 2014). Here, we  
183 calculated carbonate production, bioerosion, and net accretion rates (the percent change in  
184 volume of experimental blocks) over the one-year deployment time. In the literature, carbonate  
185 production rates on calcium carbonate blocks are typically presented as layer thickness in mm yr<sup>-1</sup>  
186 (e.g., Payri 1995, Tribollet et al. 2006), and bioerosion rates are presented as mass loss in kg m<sup>-2</sup>  
187 yr<sup>-1</sup> (e.g., Tribollet and Golubic 2005, Wisshak et al. 2012). To align our rates with literature  
188 data, these conversions were followed, but, in order to make them comparable to each other and  
189 to enable the calculation of a net rate, we used percent change in volume of the block to  
190 determine whether blocks were net accreting (positive change) or net eroding (negative change).  
191 Bioerosion and carbonate production rates were calculated using the following equations  
192 (Silbiger et al. 2016):

$$193 \quad \text{Bioerosion rate (kg m}^{-2} \text{ yr}^{-1}) = (\Delta Vol_i \times \rho_i) / (SA_i \times Time) \quad (1)$$

$$194 \quad \text{Carbonate production rate (mm yr}^{-1}) = 1000 \times (\Delta Vol_i) / (SA_i \times Time) \quad (2)$$

195 where  $i$  represents an individual block,  $\Delta Vol_i$  is the volume lost (bioerosion) or gained (carbonate  
196 production) in m<sup>3</sup>,  $SA_i$  is the surface area of the pre-deployment blocks (m<sup>2</sup>),  $\rho_i$  is the skeletal  
197 density of the pre-deployment block (kg m<sup>-3</sup>), and  $Time$  is the deployment time (years).

198 Carbonate production rates were multiplied by 1000 to convert from m to mm yr<sup>-1</sup>. Surface area  
199 was calculated from the  $\mu$ CT scans following methods by Legland et al. (2011). Skeletal density  
200 of the blocks was calculated by converting intensity values from the  $\mu$ CT scans to bulk skeletal  
201 density following methods in DeCarlo et al. (2015). Net accretion rates were calculated as  
202 percent change in volume per year (Silbiger et al. 2014):

$$203 \quad \text{Net accretion (\% y}^{-1}) = 100 \times (Vol_{post,t2} - Vol_{pre,t1}) / (Vol_{pre,t1} \times Time), \quad (3)$$

204 where  $Vol_{post,t2}$  and  $Vol_{pre,t1}$  were the post-deployment and pre-deployment volumes of the  
205 blocks, respectively. Note that this change in total volume does not depend on the alignment of  
206 pre- and post-scans.

207 **2.3 Environmental Data:** We compiled 23 variables describing the chemical, physical, and  
208 biological characteristics of each site (Table 1) from NOAA CREP

209 (<https://www.pifsc.noaa.gov/cred/>), Hawai‘i Department of Aquatic Resources (DAR), NOAA  
210 satellite data, NOAA global wave models (WaveWatch III), and *in situ* sampling. Detailed  
211 methods and collection protocols are described in the supplemental material.

## 212 **2.4 Statistical Analysis:**

213 To compare means at each level, we used a nested analysis of variance (ANOVA) with a Tukey  
214 Honestly Significant Difference (HSD) *post-hoc*, where site, island, and region were all fixed  
215 effects. To evaluate the contribution of variance at each spatial scale (sites within islands within  
216 regions) to rates of carbonate production, bioerosion, and net accretion, we used a variance  
217 components analysis, where site, island, and region were hierarchical random effects. Carbonate  
218 production and bioerosion rates were both log-transformed to meet assumptions of normality for  
219 all analyses. We used a simple linear regression to test the relationship between block skeleton  
220 density and bioerosion rates, as small differences in skeletal density on the blocks could impact  
221 bioerosion rates (Highsmith 1981a), but found no effect ( $F_{1,120} = 0.06$ ,  $p = 0.84$ ).

222 To determine environmental drivers of accretion-erosion rates, we used a model selection  
223 approach by ranking Akaike Information Criterion (AIC) weights from simple linear models in  
224 which the environmental predictors were the independent variables, and carbonate production,  
225 bioerosion, and net accretion rates were the dependent variables. All environmental data that did  
226 not meet the assumption of normality were transformed (Table 1). While it is common to find  
227 non-linear relationships in field data, we did not find any evidence of non-linearity in our dataset.  
228 AIC weights can be interpreted as a relative probability, where the model with the highest weight  
229 is the most probable of the candidate models (Wagenmakers and Farrell 2004). To test if the  
230 relationship between the environmental predictors and accretion-erosion values are consistent  
231 between regions, we constructed individual models by region and compared the highest-ranking  
232 models between regions (MHI and NWHI). A principal components analysis (PCA) was used to  
233 visualize the spatial structure of the 23 environmental parameters.

## 234 **3. RESULTS**

### 235 **3.1 Environmental drivers:**

236 The biological, chemical, and physical drivers all varied widely throughout the Hawaiian  
237 Archipelago (Fig. 2), and there were distinct patterns in environmental conditions across islands  
238 (Fig. 3).



239 *3.1.1 Biological Drivers:* Herbivorous fish biomass ranged from 0.4 to 22.8 g m<sup>-2</sup> with the  
240 highest herbivorous fish biomass on Kure in the protected Papahānaumokuākea Marine National  
241 Monument and lowest biomass on O‘ahu (Figure 2a), an island with substantial fishing pressure  
242 (Williams et al. 2008). The benthic community also fluctuated widely throughout the Hawaiian  
243 Archipelago with coral cover varying from 1.3 – 56% across the 29 sites with the lowest coral  
244 cover also on the island of O‘ahu (Fig. 2a).

245 *3.1.2. Chemical Drivers:* PO, N+N, and Si ranged from 0.008 – 0.18, 0.066 – 1.79, and 0.83 –  
246 2.45 μmol L<sup>-1</sup> (Fig. 2c), respectively, and TA, DIC, pH, and Ω<sub>arag</sub> ranged from 2197 – 2387 μmol  
247 kg<sup>-1</sup>, 1985 – 2065 μmol kg<sup>-1</sup>, 7.81 – 8.05, and 2.27 – 3.73, respectively, throughout the  
248 Archipelago (Fig. 2d,e). Lisianski, the site with the most distinct chemical environment, had the  
249 highest N+N and lowest TA, DIC, pH, and Ω<sub>arag</sub> values.

250 *3.1.3 Physical Drivers:* Average wave energy ranged from 22.3 – 45.0 kW m<sup>-2</sup> with the highest  
251 wave energy in the northernmost sites (Fig.2b). The northernmost sites also had the lowest and  
252 most variable temperatures across the archipelago with mean and standard deviation in  
253 temperature ranging from 23.4 – 25.5 °C and 0.83 – 5.25 °C, respectively (Fig.2b).

### 254 **3.2 Carbonate production, bioerosion, and net accretion rates:**

#### 255 *3.2.1 Spatial patterns in carbonate production, bioerosion and net accretion:*

256 Carbonate production, bioerosion, and net accretion rates had distinct spatial patterns  
257 throughout the Hawaiian Archipelago. At the regional scale, bioerosion rates were 39% higher at  
258 the MHI sites than at the NWHI sites (Table 2, Fig. 4b), while carbonate production rates were  
259 similar between regions (Table 2, Fig 4a); average net accretion was 2.2 times higher in the  
260 NWHI than in the MHI, but the difference was not significant (Fig. 4e and Table 2). At the  
261 island scale, however, there was significant variation in carbonate production rates, driven  
262 primarily by exceptionally high carbonate production at Lisianski (nearly double the rate of other  
263 NWHI sites; Table 2, Fig. 4d); net accretion also varied by island, with a similar pattern for  
264 Lisianski (Fig. 4f). In contrast, differences in bioerosion rate at the island scale were marginal  
265 but non-significant (Table 2, Fig. 4d). Lisianski had the highest average net accretion rate, the  
266 highest carbonate production rate, and second lowest bioerosion rate. O‘ahu, the island with the  
267 highest population density and the most direct anthropogenic impacts, had the most blocks that  
268 were net eroded (46%) and the lowest average net accretion, coupled with the second lowest  
269 carbonate production rate and highest bioerosion rate (Table S2). Lastly, site-level variation was

270 significant for all rates (Fig. 4g-i, and Table 2, S3). MauiA27 (Kahekili, Maui), a site impacted  
271 by wastewater effluent (Dailer et al. 2012), had the highest average bioerosion rate ( $0.35 \text{ kg m}^{-2}$   
272  $\text{y}^{-1} \pm 0.03$ ) and the lowest net accretion rate ( $-8.2\% \pm 1.97$ ), while LIS18 had the highest  
273 carbonate production rate ( $3.68 \pm 0.57 \text{ mm y}^{-1}$ ) (Fig. 4g-i, S2 and Table S3).

274 The variance components analysis revealed that the highest amount of variance in all  
275 three rates were at the finest spatial scales (Table 2). Regional-scale differences contributed to  
276 17.5% of the variance in bioerosion, but were negligible for carbonate production and net  
277 accretion rates whereas island-scale differences contributed to 14.5% of the variance in  
278 carbonate production, but only 2.5% in net accretion and  $<0.1\%$  in bioerosion (Table 2). Site-  
279 level differences contributed to substantially more of the variance in each rate explaining 14.9%,  
280 34.9%, and 32.1% of the variance in carbonate production, bioerosion, and net accretion rates,  
281 respectively (Table 2). However, the highest portion of variance in the data was attributed to the  
282 smallest (within sites) spatial scale, explaining 70.6%, 47.6% and 65.3% of the variance for  
283 carbonate production, bioerosion, and net accretion, respectively (Table 2).

### 284 3.2.2 Environmental drivers of carbonate production, bioerosion and net accretion:

285 Carbonate production and bioerosion rates always had different top-ranking models indicating  
286 that they respond differently to environmental conditions (Fig. 5 and Tables S4 and S5).  
287 Additionally, the environmental drivers differed between regions for all three rates (Fig. 5 and  
288 Tables S4-S6). For carbonate production, the top three models for the NWHI region were  
289 carbonate chemistry parameters; total alkalinity ranked highest and was negatively related to  
290 carbonate production ( $\text{AIC}_w = 0.40$ ,  $R^2 = 0.25$ , Fig. 5b, Table S4). Aragonite saturation state and  
291 pH had similar AIC weights and  $R^2$  values ( $\Omega_{\text{arag}}$ :  $\text{AIC}_w = 0.31$ ,  $R^2 = 0.24$ , pH:  $\text{AIC}_w = 0.28$ ,  $R^2$   
292  $= 0.24$ , Fig. 5b, Table S4) and both had a surprising negative association with carbonate  
293 production. For carbonate production in the MHI, physical and biological parameters were most  
294 parsimonious, with macroalgae ranked highest and positively associated with carbonate  
295 production ( $\text{AIC}_w = 0.30$ ,  $R^2 = 0.14$ , Fig. 5a, Table S4). For bioerosion, biological parameters  
296 were the top models in both the MHI and NWHI regions (Fig. 5c,d and Table S5); herbivore  
297 biomass was the highest-ranking model for the MHI ( $\text{AIC}_w = 0.75$ ,  $R^2 = 0.28$ , Fig 5c and Table  
298 S5), while benthic cover (% other: mainly bare substrate, cyanobacteria, and sessile  
299 invertebrates) ranked highest in the NWHI ( $\text{AIC}_w = 0.59$ ,  $R^2 = 0.11$ ; Fig. 5c and Table S5).  
300 Lastly, for net accretion, a combination of biological and chemical models was most informative

301 in both the MHI and NWHI (Fig. 5e, f and Table S6). All had relatively equal and low weights  
302 (0.16 – 0.24) and  $\Delta$ AIC values of < 4. Models ranking environmental parameters across the  
303 entire Hawaiian Archipelago are listed in Supplemental Fig 3.

## 304 **4 DISCUSSION**

### 305 ***4.1 Spatial patterns in carbonate production, bioerosion, and net accretion rates along the*** 306 ***Hawaiian Archipelago***

307 The persistence of coral reefs depends on the balance between carbonate production and  
308 net reef erosion. While several studies have examined carbonate production (or calcification) and  
309 bioerosion rates independently, this is a broad-scale study that assesses patterns in carbonate  
310 production, bioerosion, and net accretion rates in concert and compare these rates to chemical,  
311 physical, and biological drivers across spatial scales.

312 Carbonate production and bioerosion rates were associated with different drivers at both  
313 regional and archipelagic scales. Prior studies have also found distinct drivers of carbonate  
314 production and erosion: for example, a fine-scale *in situ* study showed that bioerosion was most  
315 correlated with pH while carbonate production was most correlated with distance from shore  
316 (Silbiger et al. 2016). Further, carbonate production and erosion have been shown to have  
317 different responses to the same environmental parameters, chiefly pH, in both field (Barkley et  
318 al. 2015, Enochs et al. 2016, Silbiger et al. 2016) and laboratory (Silbiger and Donahue 2015)  
319 studies. Net accretion was driven by a combination of the dominant drivers for carbonate  
320 production and bioerosion, which is expected as net accretion is a composite of carbonate  
321 production and bioerosion.

322 We were surprised that this broad-scale study did not show a strong relationship between  
323 carbonate chemistry parameters and bioerosion, as several studies show a clear relationship  
324 between pH and bioerosion (Tribollet et al. 2009, Wisshak et al. 2012, Fang et al. 2013, Reyes-  
325 Nivia et al. 2013, Wisshak et al. 2013, Silbiger et al. 2014, Barkley et al. 2015, DeCarlo et al.  
326 2015, Silbiger and Donahue 2015). Carbonate chemistry parameters were in the top-ranking  
327 models for carbonate production in the NWHI, but they also had a surprising negative  
328 relationship for both pH and  $\Omega_{\text{arag}}$ : opposite of what is expected based on prior studies (e.g.,  
329 Hoegh-Guldberg et al. 2007). In addition, nutrients were not in the top-ranking models for  
330 bioerosion, although nutrients are an important driver of reef bioerosion (e.g., Carreiro-Silva et  
331 al. 2005, DeCarlo et al. 2015). Silica, however, was in the top three models for bioerosion in

332 both regions. Excavating sponges have a siliceous skeleton; thus, sponge bioerosion rates could  
333 be sensitive to silica concentrations. There are a few possible explanations for these surprising  
334 results in the chemical parameters. 1) It is likely other, unmeasured collinear parameters are  
335 driving the negative relationship between carbonate production and pH. 2) All reef sites for  
336 which we had nutrient data were oligotrophic ( $0.066 - 1.8 \mu\text{mol L}^{-1}$ ); thus, the range of nitrate  
337 was inadequate to elicit a nutrient response in bioerosion. 3) Nutrient data was unavailable for  
338 site with the highest bioerosion rates (Kahekili, Maui – Maui A27); a site known to be impacted  
339 by wastewater effluent (Dailer et al. 2012) and likely with high nutrient concentrations. 4) The  
340 chemistry data had low replication (1-3 points) collected between spring and summer during  
341 daylight hours which ignores the high temporal variability in water chemistry on coral reefs (e.g.,  
342 Guadayol et al. 2014). Prior studies have shown that diel variability in carbonate chemistry is an  
343 important driver of carbonate production on coral reefs (Price et al. 2012). This low replication  
344 reflects the only data publicly available for these very remote sites. However, a previous study  
345 over broad spatial scales used similarly sparse *in situ* chemistry data and found significant  
346 relationships between bioerosion and water chemistry (DeCarlo et al. 2015). 5) The strong direct  
347 and indirect effects of herbivore grazing may be swamping or interacting with the effects  
348 carbonate chemistry and nutrients on bioerosion rates. Overall, the drivers of accretion-erosion  
349 rates were multifactorial, highlighting the many interacting factors that influence accretion-  
350 erosion rates of coral reefs.

351 Biological parameters ranked highest in five out of the six model selection analyses.  
352 Specifically, herbivorous fish was the highest-ranking model in the MHI for bioerosion, and  
353 benthic cover descriptors ranked highest for carbonate production in the MHI, bioerosion in the  
354 NWHI, and net accretion in both regions. Benthic cover, specifically the amount of dead  
355 substrate on a reef, could influence bioerosion rates, as bioeroders prefer dead substrate over live  
356 reef (Highsmith 1981b, Hutchings 1986). Herbivorous fish can directly influence bioerosion by  
357 removing  $\text{CaCO}_3$  substrate while grazing for algae (e.g., Bellwood 1995, Ong and Holland  
358 2010), and they can indirectly influence settlement and growth of calcifiers by removing fleshy  
359 algae and relieving competitive interactions with CCA (Cebrian and Uriz 2006, Cebrian 2010,  
360 O'Leary and McClanahan 2010, González-Rivero et al. 2012). Further, the interaction between  
361 benthic community composition and herbivorous fish can influence bioerosion rates because the  
362 presence of secondary calcifiers, mainly CCA, can inhibit the settlement of bioeroders by sealing

363 off the substrate and making it difficult for borers to penetrate (White 1980, Tribollet and Payri  
364 2001). A prior field study suggested that grazer abundance could mediate the relationship  
365 between accretion and pH as they saw a positive relationship between pH and accretion at one  
366 CO<sub>2</sub> vent site and no relationship at a site with higher grazer abundance (Enochs et al. 2016).  
367 Our results suggest that herbivorous fish have a negative indirect effect on bioerosion rates:  
368 bioerosion rates decreased with increasing herbivorous fish biomass. The strong negative effect  
369 of herbivorous fish biomass on bioerosion rates is important for coral reef managers: managing  
370 for herbivorous fish could mitigate excessive bioerosion.

371 Among the physical parameters, mean and maximum SST were in the top-ranking  
372 models for carbonate production in the MHI. Carbonate production can vary as a function of  
373 temperature due to its effects on both chemical and biological processes (Mutti and Hallock  
374 2003). Across all models, the top five highest-ranking models often had  $\Delta$ AIC values of <4  
375 (Table S4-S6), indicating empirical support for several of the environmental parameters and,  
376 thus, evidence for multiple factors interacting to affect the accretion-erosion balance of coral  
377 reefs.

378 In addition to different drivers between carbonate production and erosion rates, the  
379 dominant drivers for carbonate production, bioerosion, and net accretion were always different  
380 between the two regions. There are several possible explanations for these differences. First,  
381 there are different ranges in the environmental parameters due to varying oceanographic  
382 conditions and human-influences between the two regions. For example, there was a much larger  
383 range in the carbonate chemistry in the NWHI than in the MHI which was mostly driven by  
384 Lisianski Island (Fig. 2d,e, 3a). Interestingly, Lisianski also had a substantially higher carbonate  
385 production rate than the five other islands/atolls (Fig. 4a). Unlike other atolls in the NWHI,  
386 Lisianski is an open atoll with reticulate reef separating lagoon and forereefs; this unique  
387 geomorphology may underlie the distinct physicochemical environment (Fig 3a) and carbonate  
388 production rates (Fig 4b) at Lisianski. There were considerable differences in fish biomass  
389 between the two regions due to varying fishing pressure (Williams et al. 2008, Williams et al.  
390 2010), likely driving the difference in the relative importance of herbivorous fish between the  
391 MHI and NWHI. Prior studies have also found dissimilar relationships between environmental  
392 drivers and coral reef processes between regions. For example, a Pacific Basin study  
393 demonstrated that the relationship between environmental models and reef characteristics (coral,

394 CCA, and macroalgal cover) were not consistent across space (Williams et al. 2015). Williams et  
395 al. (2015) split sites between populated and unpopulated islands, found that biophysical  
396 parameters had higher explanatory power at unpopulated islands, and concluded that local  
397 human impacts decouple biophysical relationships on coral reefs. The MHI versus NWHI  
398 comparison is similarly populated versus unpopulated, and differences between sites could be  
399 driven by local human impacts; however, there are also several other major differences between  
400 these regions that may be more directly related (e.g., high vs low islands, benthic habitat  
401 differences, etc.).

402         Variability in carbonate production, bioerosion, and net accretion were all highest at the  
403 local scale. For all factors investigated here, the smallest scale of variation (within sites)  
404 contributed much more variance than any other spatial scale in this study, indicating that  
405 individual blocks within a site were more different than blocks 2500 km apart. It is important to  
406 note that the site scale is the residual variance and, therefore, includes all block-to-block  
407 variability within a site, including both spatial variability within each site and any differences  
408 between the blocks themselves. While our rate calculations normalized for differences between  
409 blocks in volume and surface area, and we found no effect of skeletal density, other differences  
410 between blocks, such as differences in surface roughness, or variability in the  $\mu$ CT  
411 measurements, would also contribute to within-site variability. Prior studies have also seen  
412 exceptionally high within-site variability in bioerosion rates. A recent study in Kāneʻohe Bay,  
413 Hawaiʻi saw a nearly 2 order of magnitude change in bioerosion rates across a short 34-m  
414 transect (Silbiger et al. 2016) – variability that was greater than a study comparing bioerosion  
415 rates across the Pacific (DeCarlo et al. 2015). Further, the low explanatory power of all  
416 environmental models (highest  $R^2$  value was 0.28) reflect a response to the high local variability  
417 in accretion-erosion data. Prior studies examining within site environmental variability and  
418 accretion-erosion rates had markedly higher explanatory power between accretion-erosion rates  
419 and environmental parameters (Silbiger et al. 2014, Silbiger et al. 2016). While both broad and  
420 local scale gradients in biological and physicochemical drivers clearly interact to shape patterns  
421 in the accretion-erosion balance, this study provides compelling evidence that local variability is  
422 particularly important.

423         There are some limitations to this study that should be considered when interpreting the  
424 results. First, the temporal scales of the environmental variables differ and, particularly in the

425 case of water chemistry, are disconnected from the block deployment period (Table S1 and S7).  
426 Second, the highest spatial resolution of the environmental data was at the site level, but the  
427 majority of the variance in the accretion-erosion data was within sites. Monitoring protocols are  
428 typically in place to track broad environmental trends; however, a better understanding of local-  
429 scale variability is necessary to predict how environmental change will impact the accretion-  
430 erosion balance. Third, because the blocks were deployed for one year, the results are based on  
431 an early successional community. Studies have shown that bioeroder community composition  
432 and bioerosion rates change over time in CaCO<sub>3</sub> block experiments (e.g., Hutchings et al. 1992,  
433 Tribollet and Golubic 2005). For example, several species of boring polychaetes have shown  
434 increased recruitment over a one to two-year deployment period followed by a decline, while  
435 eunicids, sipunculans, and bivalves continuously increased over a four-year period in Australia  
436 (Hutchings et al. 1992). Another study demonstrated that bioerosion rates on Lizard Island,  
437 Australia were 0.71, 0.11, and 0.32 kg m<sup>-2</sup> y<sup>-1</sup> after a one-year exposure for microborers,  
438 macroborers, and grazers, respectively. After 3 years of exposure, macrobioerosion rates were 3x  
439 higher (Tribollet and Golubic 2005). As bioeroding species respond differently to environmental  
440 conditions and erode at different rates (e.g., Hutchings 1986, Hutchings et al. 1992, Hutchings  
441 and Peyrot-Clausade 2002, Tribollet and Golubic 2005), the deployment length could have  
442 impacted the results of this study. Lastly, our analysis did not separate bioerosion rates by  
443 functional groups. Future studies should address the effect of multiple chemical, physical, and  
444 biological divers of bioerosion functional groups at multiple successional stages.

#### 445 **4.2 Conclusions**

446 Despite the limitations, this is the highest resolution analysis that allows for the  
447 simultaneous measurement of carbonate production, bioerosion, and net accretion from the same  
448 experimental substrate and correlates these rates with a suite of chemical, physical, and  
449 biological parameters, and the first study to use  $\mu$ CT to quantify carbonate production,  
450 bioerosion and net accretion rates over large spatial scales. Our results and those from previous  
451 studies (Silbiger et al. 2014, Silbiger et al. 2016) provide compelling evidence that local-scale  
452 environmental variability is particularly important to the coral reef accretion-erosion balance. We  
453 also demonstrated that the relationships between explanatory and response variables are not  
454 consistent across space, as there were differences in the highest-ranking environmental models  
455 between the MHI and NWHI datasets. The differing relationships between environmental

456 variability and accretion-erosion data should be taken into consideration when interpreting those  
457 results and in future management decisions on coral reefs.

458 **ACKNOWLEDGMENTS:**

459 We thank NOAA's Coral Reef Ecosystem Program and the Hawaii Division of Aquatic  
460 Resources for providing most of the environmental data. Field help and logistical support was  
461 provided by several NOAA employees and the crew of NOAA ship Hi'ialakai. In particular, we  
462 thank C. Richards, M. Timmers, C. Young, I. Williams, J. Caldwell, M. Walton, J. Burns, C.  
463 Counsell, E. Nalley, J. Zill, R. Toonen, R. Coleman, G. Stender, J. Jones, M. Royer, J. Whitney,  
464 S. Godwin, H. Bolick, and E.M. Sogin. This project was supported by the NOAA Nancy Foster  
465 Scholarship Program to NJS, the HIMB-NWHI Partnership Program to MJD, the Jessie D Kay  
466 Memorial Fellowship to NJS, and the University of Hawaii SeaGrant Program to MJD. This  
467 paper is funded in part by a grant/cooperative agreement from the National Oceanic and  
468 Atmospheric Administration, Project No. R/IR-18, which is sponsored by the University of  
469 Hawai'i Sea Grant College Program, School of Ocean and Earth Science and Technology, under  
470 Institutional Grant No. NA09OAR4170060 Office of Sea Grant, Department of Commerce. The  
471 views expressed herein are those of the authors and do not necessarily reflect the views of  
472 NOAA or any of its subagencies. This is SeaGrant contribution UNIHI-SEAGRANT-JC-14-52  
473 and HIMB # XXXX.

474 **REFERENCES:**

- 475 Barkley, H. C., A. L. Cohen, Y. Golbuu, V. R. Starczak, T. M. DeCarlo, and K. E. F.  
476 Shamberger. 2015. Changes in coral reef communities across a natural gradient in  
477 seawater pH. *Science advances* **1**:e1500328.
- 478 Bellwood, D. R. 1995. Direct estimate of bioerosion by two parrotfish species, *Chlorurus gibbus*  
479 and *C. sordidus*, on the Great Barrier Reef, Australia. *Marine Biology* **121**:419-429.
- 480 Brown-Saracino, J., P. Peckol, H. A. Curran, and M. L. Robbart. 2007. Spatial variation in sea  
481 urchins, fish predators, and bioerosion rates on coral reefs of Belize. *Coral Reefs* **26**:71-  
482 78.
- 483 Bruno, J. F., and E. R. Selig. 2007. Regional decline of coral cover in the Indo-Pacific: timing,  
484 extent, and subregional comparisons. *PloS one* **2**:e711.



- 485 Carreiro-Silva, M., T. R. McClanahan, and W. E. Kiene. 2005. The role of inorganic nutrients  
486 and herbivory in controlling microbioerosion of carbonate substratum. *Coral Reefs*  
487 **24**:214-221.
- 488 Cebrian, E. 2010. Grazing on coral reefs facilitates growth of the excavating sponge *Cliona*  
489 *orientalis* (Clionidae, Hadromerida). *Marine Ecology* **31**:533-538.
- 490 Cebrian, E., and M. J. Uriz. 2006. Grazing on fleshy seaweeds by sea urchins facilitates sponge  
491 *Cliona viridis* growth. *Marine Ecology Progress Series* **323**:83-89.
- 492 Comeau, S., P. J. Edmunds, N. B. Spindel, and R. C. Carpenter. 2013. The responses of eight  
493 coral reef calcifiers to increasing partial pressure of CO<sub>2</sub> do not exhibit a tipping point.  
494 *Limnology and Oceanography* **58**:388-398.
- 495 Dailer, M. L., H. L. Ramey, S. Saephan, and C. M. Smith. 2012. Algal δ 15 N values detect a  
496 wastewater effluent plume in nearshore and offshore surface waters and three-  
497 dimensionally model the plume across a coral reef on Maui, Hawai 'i, USA. *Marine*  
498 *Pollution Bulletin* **64**:207-213.
- 499 Davies, P. J., and P. A. Hutchings. 1983. Initial colonization, erosion and accretion on coral  
500 substrate: experimental results. Lizard Island Great Barrier Reef. *Coral Reefs* **2**:27-35.
- 501 DeCarlo, T. M., A. L. Cohen, H. C. Barkley, Q. Cobban, C. Young, K. E. Shamberger, R. E.  
502 Brainard, and Y. Golbuu. 2015. Coral macrobioerosion is accelerated by ocean  
503 acidification and nutrients. *Geology* **43**:7-10.
- 504 Diaz-Pulido, G., K. Anthony, D. I. Kline, S. Dove, and O. Hoegh- Guldberg. 2012. Interactions  
505 between ocean acidification and warming on the mortality and dissolution of coralline  
506 alge. *Journal of Phycology* **48**:32-39.
- 507 Enochs, I. C., D. P. Manzello, R. D. Carlton, D. M. Graham, R. Ruzicka, and M. A. Colella.  
508 2015. Ocean acidification enhances the bioerosion of a common coral reef sponge:  
509 implications for the persistence of the Florida Reef Tract. *Bulletin of Marine Science*  
510 **91**:271-290.
- 511 Enochs, I. C., D. P. Manzello, G. Kolodziej, S. H. C. Noonan, L. Valentino, and K. E. Fabricius.  
512 2016. Enhanced macroboring and depressed calcification drive net dissolution at high-  
513 CO<sub>2</sub> coral reefs. **283**:20161742.
- 514 Fabricius, K. E. 2005. Effects of terrestrial runoff on the ecology of corals and coral reefs:  
515 review and synthesis. *Marine Pollution Bulletin* **50**:125-146.

- 516 Fang, J. K. H., M. A. Mello-Athayde, C. H. L. Schönberg, D. I. Kline, O. Hoegh-Guldberg,  
517 and S. Dove. 2013. Sponge biomass and bioerosion rates increase under ocean warming  
518 and acidification. *Global Change Biology* **19**:3581-3591.
- 519 Gardner, T. A., I. M. Côté, J. A. Gill, A. Grant, and A. R. Watkinson. 2003. Long-term region-  
520 wide declines in Caribbean corals. *Science* **301**:958-960.
- 521 González-Rivero, M., R. Ferrari, C. H. L. Schönberg, and P. J. Mumby. 2012. Impacts of  
522 macroalgal competition and parrotfish predation on the growth of a common bioeroding  
523 sponge. *Marine Ecology Progress Series* **444**:133-142.
- 524 Guadayol, Ó., N. J. Silbiger, M. J. Donahue, and F. I. M. Thomas. 2014. Patterns in temporal  
525 variability of temperature, oxygen and pH along an environmental gradient in a coral  
526 reef. *PloS one* **9**:e85213.
- 527 Hamylton, S. M., A. Pescud, J. X. Leon, and D. P. Callaghan. 2013. A geospatial assessment of  
528 the relationship between reef flat community calcium carbonate production and wave  
529 energy. *Coral Reefs* **32**:1025-1039.
- 530 Hearn, C., M. Atkinson, and J. Falter. 2001. A physical derivation of nutrient-uptake rates in  
531 coral reefs: effects of roughness and waves. *Coral Reefs* **20**:347-356.
- 532 Highsmith, R. C. 1981a. Coral bioerosion - damage relative to skeletal density. *American*  
533 *Naturalist* **117**:193-198.
- 534 Highsmith, R. C. 1981b. Coral bioerosion at Enewetak- agents and dynamics. *Internationale*  
535 *Revue Der Gesamten Hydrobiologie* **66**:335-375.
- 536 Hoegh-Guldberg, O., P. J. Mumby, A. J. Hooten, R. S. Steneck, P. Greenfield, E. Gomez, C. D.  
537 Harvell, P. F. Sale, A. J. Edwards, K. Caldeira, N. Knowlton, C. M. Eakin, R. Iglesias-  
538 Prieto, N. Muthiga, R. H. Bradbury, A. Dubi, and M. E. Hatziolos. 2007. Coral reefs  
539 under rapid climate change and ocean acidification. *Science* **318**:1737-1742.
- 540 Hutchings, P. 2011. Bioerosion. Pages 139-156 *Encyclopedia of Modern Coral Reefs*. Springer.
- 541 Hutchings, P., M. Peyrot-Clausade, and A. Osnorno. 2005. Influence of land runoff on rates and  
542 agents of bioerosion of coral substrates. *Marine Pollution Bulletin* **51**:438-447.
- 543 Hutchings, P. A. 1986. Biological destruction of coral reefs- a review. *Coral Reefs* **4**:239-252.
- 544 Hutchings, P. A., W. E. Kiene, R. B. Cunningham, and C. Donnelly. 1992. Spatial and temporal  
545 patterns of non-colonial boring organisms (Polychaetes, Sipunculans and Bivalve  
546 molluscs) in *Porites* at Lizard Island, Great Barrier Reef. *Coral Reefs* **11**:23-31.

- 547 Hutchings, P. A., and M. Peyrot-Clausade. 2002. The distribution and abundance of boring  
548 species of polychaetes and sipunculans in coral substrates in French Polynesia. *Journal of*  
549 *Experimental Marine Biology and Ecology* **269**:101-121.
- 550 Johnson, M. D., and R. C. Carpenter. 2012. Ocean acidification and warming decrease  
551 calcification in the crustose coralline alga *Hydrolithon onkodes* and increase  
552 susceptibility to grazing. *Journal of Experimental Marine Biology and Ecology* **434**:94-  
553 101.
- 554 Jokiel, P. L., K. S. Rodgers, I. B. Kuffner, A. J. Andersson, E. F. Cox, and F. T. Mackenzie.  
555 2008. Ocean acidification and calcifying reef organisms: a mesocosm investigation. *Coral*  
556 *Reefs* **27**:473-483.
- 557 Jury, C. P., F. I. M. Thomas, M. J. Atkinson, and R. J. Toonen. 2013. Buffer capacity, ecosystem  
558 feedbacks, and seawater chemistry under global change. *Water* **5**:1303-1325.
- 559 Kennedy, E. V., C. T. Perry, P. R. Halloran, R. Iglesias-Prieto, C. H. L. Schönberg, M. Wisshak,  
560 A. U. Form, J. P. Carricart-Ganivet, M. Fine, and C. M. Eakin. 2013. Avoiding coral reef  
561 functional collapse requires local and global action. *Current Biology* **23**:912-918.
- 562 Le Grand, H. M., and K. E. Fabricius. 2011. Relationship of internal macrobioeroder densities in  
563 living massive *Porites* to turbidity and chlorophyll on the Australian Great Barrier Reef.  
564 *Coral Reefs* **30**:97-107.
- 565 Legland, D., K. Kiêu, and M.-F. Devaux. 2011. Computation of Minkowski measures on 2D and  
566 3D binary images. *Image Analysis & Stereology* **26**:83-92.
- 567 Madin, J. S., and S. R. Connolly. 2006. Ecological consequences of major hydrodynamic  
568 disturbances on coral reefs. *Nature* **444**:477-480.
- 569 Mutti, M., and P. Hallock. 2003. Carbonate systems along nutrient and temperature gradients:  
570 some sedimentological and geochemical constraints. *International Journal of Earth*  
571 *Sciences* **92**:465-475.
- 572 Neumann, A. C. 1966. Observations on coastal erosion in Bermuda and measurements of boring  
573 rate of sponge *Cliona lampa*. *Limnology and Oceanography* **11**:92-108.
- 574 O'Leary, J. K., and T. R. McClanahan. 2010. Trophic cascades result in large-scale coralline  
575 algae loss through differential grazer effects. *Ecology* **91**:3584-3597.
- 576 Ong, L., and K. N. Holland. 2010. Bioerosion of coral reefs by two Hawaiian parrotfishes:  
577 species, size differences and fishery implications. *Marine Biology* **157**:1313-1323.

- 578 Payri, C. E. 1995. Production carbonatée de quelques algues calcifiées sur un récif corallien de  
579 Polynésie française. Bulletin de la Societe Geologique de France **166**:77-84.
- 580 Perry, C. T., E. N. Edinger, P. S. Kench, G. N. Murphy, S. G. Smithers, R. S. Steneck, and P. J.  
581 Mumby. 2012. Estimating rates of biologically driven coral reef framework production  
582 and erosion: a new census-based carbonate budget methodology and applications to the  
583 reefs of Bonaire. Coral Reefs **31**:1-16.
- 584 Price, N. N., T. R. Martz, R. E. Brainard, and J. E. Smith. 2012. Diel variability in seawater pH  
585 relates to calcification and benthic community structure on coral reefs. PloS one  
586 **7**:e43843-e43843.
- 587 Reyes-Nivia, C., G. Diaz-Pulido, D. Kline, O.-H. Guldborg, and S. Dove. 2013. Ocean  
588 acidification and warming scenarios increase microbioerosion of coral skeletons. Global  
589 Change Biology **19**:1919-1929.
- 590 Risk, M. J., P. W. Sammarco, and E. N. Edinger. 1995. Bioerosion in *Acropora* across the  
591 continental shelf of the Great Barrier Reef. Coral reefs **14**:79-86.
- 592 Rützler, K. 1975. The role of burrowing sponges in bioerosion. Oecologia **19**:203-216.
- 593 Scott, P. J. B., and M. J. Risk. 1988. The effect of Lithophaga (Bivalvia, Mytilidae) boreholes on  
594 the strength of the coral *Porites lobata*. Coral Reefs **7**:145-151.
- 595 Silbiger, N. J., and M. J. Donahue. 2015. Secondary calcification and dissolution respond  
596 differently to future ocean conditions. Biogeosciences **12**:567-578.
- 597 Silbiger, N. J., Ò. Guadayol, F. I. M. Thomas, and M. J. Donahue. 2014. Reefs shift from net  
598 accretion to net erosion along a natural environmental gradient. Marine Ecology Progress  
599 Series **515**:33-44.
- 600 Silbiger, N. J., Ò. Guadayol, F. I. M. Thomas, and M. J. Donahue. 2016. A novel  $\mu$ CT analysis  
601 reveals different responses of bioerosion and secondary accretion to environmental  
602 variability. PloS one **11**:e0153058.
- 603 Tribollet, A., G. Decherf, P. A. Hutchings, and M. Peyrot-Clausade. 2002. Large-scale spatial  
604 variability in bioerosion of experimental coral substrates on the Great Barrier Reef  
605 (Australia): importance of microborers. Coral Reefs **21**:424-432.
- 606 Tribollet, A., C. Godinot, M. Atkinson, and C. Langdon. 2009. Effects of elevated  $p\text{CO}_2$  on  
607 dissolution of coral carbonates by microbial euendoliths. Global Biogeochemical Cycles  
608 **23**:GB3008.

- 609 Tribollet, A., and S. Golubic. 2005. Cross-shelf differences in the pattern and pace of bioerosion  
610 of experimental carbonate substrates exposed for 3 years on the northern Great Barrier  
611 Reef, Australia. *Coral Reefs* **24**:422-434.
- 612 Tribollet, A., and S. Golubic. 2011. Reef bioerosion: agents and processes. Pages 435-449 *Coral*  
613 *reefs: An ecosystem in transition*. Springer.
- 614 Tribollet, A., C. Langdon, S. Golubic, and M. Atkinson. 2006. Endolithic microflora are major  
615 primary producers in dead carbonate substrates of Hawaiian coral reefs. *Journal of*  
616 *Phycology* **42**:292-303.
- 617 Tribollet, A., and C. Payri. 2001. Bioerosion of the coralline alga *Hydrolithon onkodes* by  
618 microborers in the coral reefs of Moorea, French Polynesia. *Oceanologica Acta* **24**:329-  
619 342.
- 620 Wagenmakers, E.-J., and S. Farrell. 2004. AIC model selection using Akaike weights.  
621 *Psychonomic bulletin & review* **11**:192-196.
- 622 White, J. 1980. Distribution, recruitment and development of the borer community in dead coral  
623 on shallow Hawaiian reefs. University of Hawaii at Manoa, Honolulu.
- 624 Williams, G. J., J. M. Gove, Y. Eynaud, B. J. Zgliczynski, and S. A. Sandin. 2015. Local human  
625 impacts decouple natural biophysical relationships on Pacific coral reefs. *Ecography*.
- 626 Williams, I. D., B. L. Richards, S. A. Sandin, J. K. Baum, R. E. Schroeder, M. O. Nadon, B.  
627 Zgliczynski, P. Craig, J. L. McIlwain, and R. E. Brainard. 2010. Differences in reef fish  
628 assemblages between populated and remote reefs spanning multiple archipelagos across  
629 the central and western Pacific. *Journal of Marine Biology* **2011**:1-14.
- 630 Williams, I. D., W. J. Walsh, R. E. Schroeder, A. M. Friedlander, B. L. Richards, and K. A.  
631 Stamoulis. 2008. Assessing the importance of fishing impacts on Hawaiian coral reef fish  
632 assemblages along regional-scale human population gradients. *Environmental*  
633 *Conservation* **35**:261-272.
- 634 Wisshak, M., C. H. L. Schönberg, A. Form, and A. Freiwald. 2012. Ocean acidification  
635 accelerates reef bioerosion. *Plos One* **7**:e45124-e45124.
- 636 Wisshak, M., C. H. L. Schönberg, A. Form, and A. Freiwald. 2013. Effects of ocean acidification  
637 and global warming on reef bioerosion—lessons from a clionaid sponge. *Aquatic Biology*  
638 **19**:111-127.
- 639

640

641

642

643

644 **Data Accessibility**

645 Data are available on GitHub: <https://doi.org/10.5281/zenodo.818093>

Author Manuscript

Table 1: Environmental parameters: Environmental parameters grouped by (a) chemical, (b) physical, (c) and biological drivers.

Parameters are parameter type, transformation is how the data were normalized, data source is the agency, satellite, or model source for the data, and method is collection method for each parameter.

Parameters	Abbreviation	Transformation	Data Source	Method
<b>(a) Chemical</b>				
PO <sub>4</sub> <sup>3-</sup>	PO	log(X)	CREP/Silbiger <sup>1</sup>	Water Sample
Si	Si	log(X)	CREP/Silbiger <sup>1</sup>	Water Sample
NO <sub>3</sub> <sup>-</sup> + NO <sub>2</sub> <sup>-</sup>	N+N	log(X)	CREP/Silbiger <sup>1</sup>	Water Sample
Ω <sub>arag</sub>	Ω <sub>arag</sub>	log(X)	CREP/Silbiger <sup>1</sup>	CO2SYS
pH	pH	log(X)	CREP/Silbiger <sup>1</sup>	CO2SYS
Total Alkalinity (salinity normalized)	TA	log(X)	CREP/Silbiger <sup>1</sup>	Water Sample
Dissolved Inorganic Carbon (salinity normalized)	DIC	log(X)	CREP/Silbiger <sup>1</sup>	Water Sample
<b>(b) Physical</b>				
Depth	Depth	NA	CREP	Dive computer
Mean Sea Surface Temperature	mean(SST)	NA	G1SST	Satellite
Maximum Sea Surface Temperature	max(SST)	NA	G1SST	Satellite
Minimum Sea Surface Temperature	min(SST)	NA	G1SST	Satellite
Standard Deviation of Sea Surface Temperature	std(SST)	log(X)	G1SST	Satellite
Mean Wave Energy	mean(energy)	log(X)	Wave Watch III	Satellite
Maximum Wave Energy	max(energy)	log(X)	Wave Watch III	Satellite
Sum of Wave Energy	sum(energy)	NA	Wave Watch III	Satellite
Standard Deviation Wave Energy	std(energy)	log(X)	Wave Watch III	Satellite
<b>(c) Biological</b>				
Fish herbivore biomass	Herb	log(X)	CREP/DAR <sup>2</sup>	BLT/nSPC
% Coral cover	% Coral	log(X+1)	CREP/DAR <sup>2</sup>	LPI/Photoquad <sup>3</sup>

% Calcified algae	% Calg	log(X+1)	CREP/DAR <sup>2</sup>	LPI/Photoquad <sup>3</sup>
% Macroalgae	% Malg	log(X+1)	CREP/DAR <sup>2</sup>	LPI/Photoquad <sup>3</sup>
% Turf algae	% Talg	log(X+1)	CREP/DAR <sup>2</sup>	LPI/Photoquad <sup>3</sup>
% Sand	% Sand	log(X+1)	CREP/DAR <sup>2</sup>	LPI/Photoquad <sup>3</sup>
% Other	% Other	log(X+1)	CREP/DAR <sup>2</sup>	LPI/Photoquad <sup>3</sup>

<sup>1.</sup> Silbiger collected nutrient samples at all O‘ahu sites and carbonate chemistry samples at all Maui sites and OahuKB and OahuKN. All other data was collected by CREP. There is currently no nutrient data available for MauiA27

<sup>2.</sup> MauiA27 fish and benthic data was collected by DAR and all other data was collected by CREP

<sup>3.</sup> Data was collected using LPI at all sites except for OahuKBay, OahuKN, Oahu10, Oahu4, and MauiA27

Table 2: Hierarchical ANOVA for (a) carbonate production, (b) bioerosion, and (c) net accretion rates across regions, islands, and sites. DF is degrees of freedom, SS is sum of squares, Mean SS is mean sum of squares, F is the F-test, and p is the p-value. Percent variance is from a variance components analysis, where site, island, and region were hierarchical random effects. Bold values represent statistically significant differences.

Model	DF	SS	Mean SS	F	p	% Variance
a) Carbonate Production						
Region	1	0.025	0.25	1.26	0.27	<0.1%
Island:Region	4	5.48	1.37	7.03	<b>&lt;0.001</b>	14.50%
Site:Island:Region	23	8.55	0.37	1.91	<b>0.01</b>	14.90%
Residuals/Within Site	93	18.11	0.19			70.60%
b) Bioerosion						



Region	1	7.15	7.15	20.18	<b>&lt;0.001</b>	17.50%
Island:Region	4	3.41	0.85	2.4	0.055	<0.1%
Site:Island:Region	23	35.6	1.55	4.37	<b>&lt;0.001</b>	34.90%
Residuals/Within Site	93	32.96	0.35			47.60%
c) Net Accretion						
Region	1	65.1	65.14	2.76	0.1	<0.1%
Island:Region	4	374.2	93.56	3.97	<b>0.005</b>	2.50%
Site:Island:Region	21	1641.7	71.38	3.03	<b>&lt;0.001</b>	32.10%
Residuals/Within Site	93	2215.1	23.57			65.30%

Author Manuscript

646 Figure Legend:

647 **Figure 1: Map of 29 forereef sites across the Hawaiian Archipelago.** Top inset shows the  
648 extent of the Hawaiian Archipelago. Maui and O‘ahu are in the Main Hawaiian Islands region  
649 and French Frigate Shoals, Lisianski Atoll, Pearl and Hermes Atoll, and Kure Atoll are in the  
650 Northwestern Hawaiian Islands region in the Papāhānaumokuākea Marine National Monument.  
651 Green areas are land. Red dots are individual sites. Grey areas in maps are 0-40m bathymetry  
652 data from NOAA CREP.

653  
654 **Figure 2: Summary of environmental data for (a) biological, (b) physical, and (c-e)**  
655 **chemical drivers.** (a) Benthic cover is the mean % cover of the benthic community for all data  
656 collected between 2010 – 2012 at each site. (a) Herbivore fish biomass ( $\text{g m}^{-2}$ ) are the means  $\pm$   
657 SE for all available data between 2000 – 2014 at each site. In the physical data plot (b), black  
658 and red bars represent the ranges for temperature ( $^{\circ}\text{C}$ ) and wave energy ( $\text{kW m}^{-2}$ ), respectively,  
659 and the dots are the mean values. The chemistry plots show mean values for (c) PO, Si, and N+N  
660 in  $\mu\text{mol L}^{-1}$ , (d) TA ( $\mu\text{Eq kg}^{-1}$ ), DIC ( $\mu\text{mol kg}^{-1}$ ), and  $\Omega_{\text{arag}}$  (colors), and (e) pH for all data  
661 available between 2008 – 2014 at each site. The sites are ordered from south to north. All  
662 parameters and data sources are listed in Table 1.

663  
664 **Figure 3: Principal components analysis (PCA) of the environmental data.** The PCA is a  
665 combination of all environmental parameters collected (Table 1). Panel (a) are the PC scores of  
666 each site and panel (b) are the loadings of each environmental parameter. The x-axis is the first  
667 principal component and y-axis is the second principal component. Numbers in parentheses are  
668 the percent of variance explained by each PC axis. Polygons outline data from individual islands.

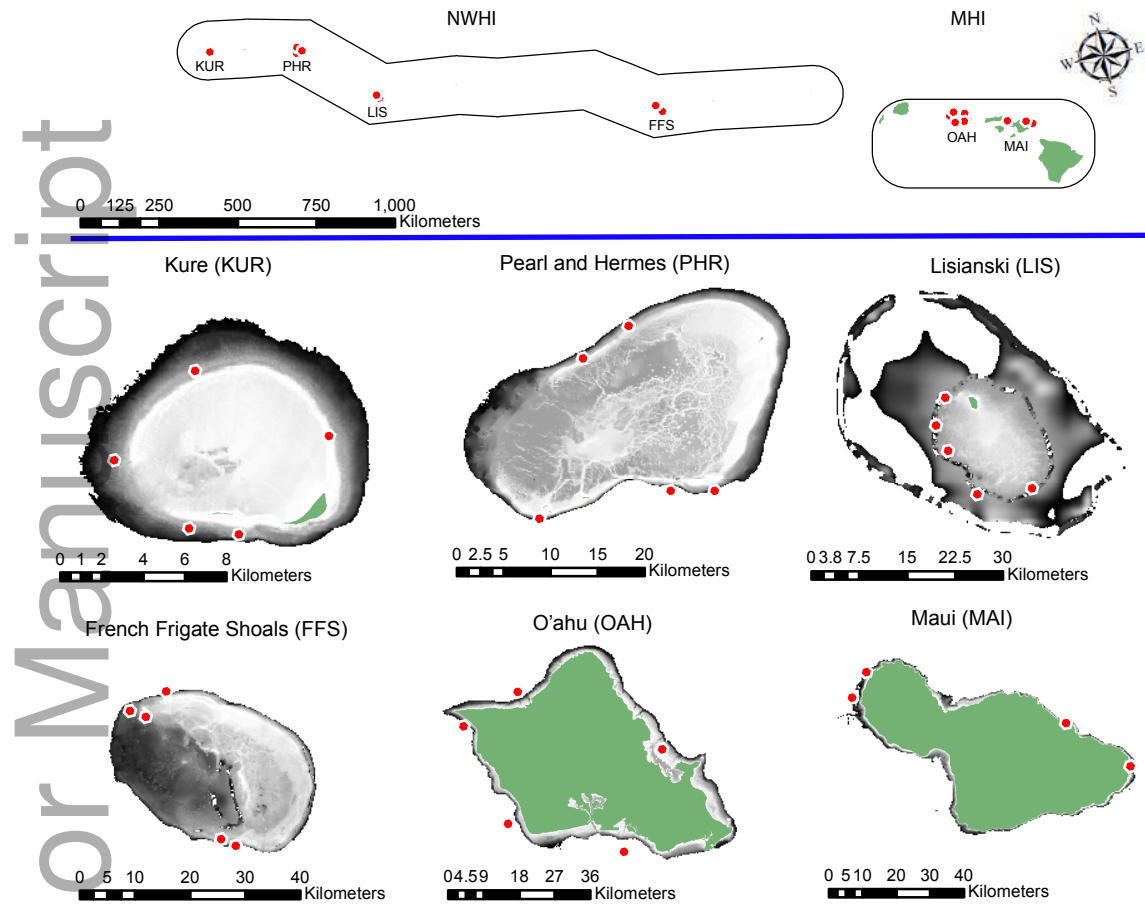
669  
670 **Figure 4: Means  $\pm$  SE for (a,d,g) carbonate production, (b,e,h) bioerosion, and (c,f,i) net**  
671 **accretion rates across (a,b,c) regions, (d,e,f) islands, and sites (g,h,i).** For net accretion,  
672 positive values were net accreting while sites with negative values were net eroding over the  
673 deployment period. Sites are show in order of latitude. Data were log-transformed in the analysis  
674 and were back-transformed in this figure. ANOVA results for this figure are in Table 2. Letters  
675 are from pairwise comparisons from a TukeyHSD post-hoc test and means with different letters

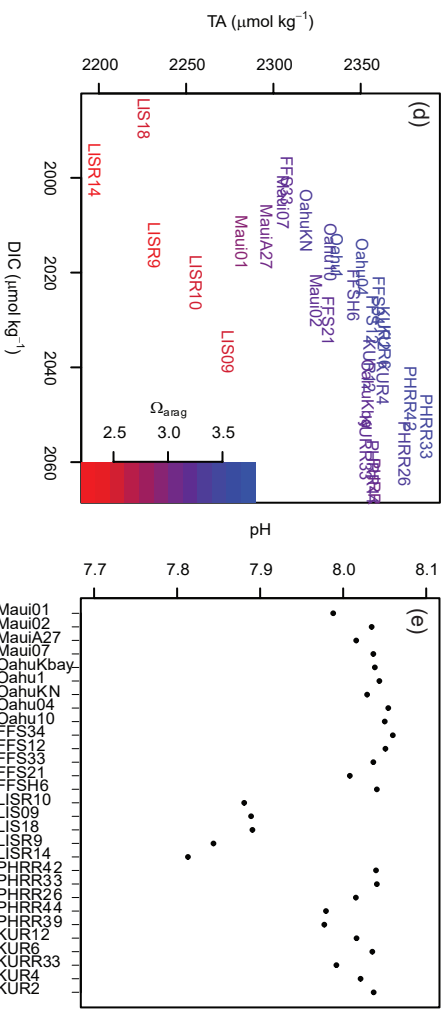
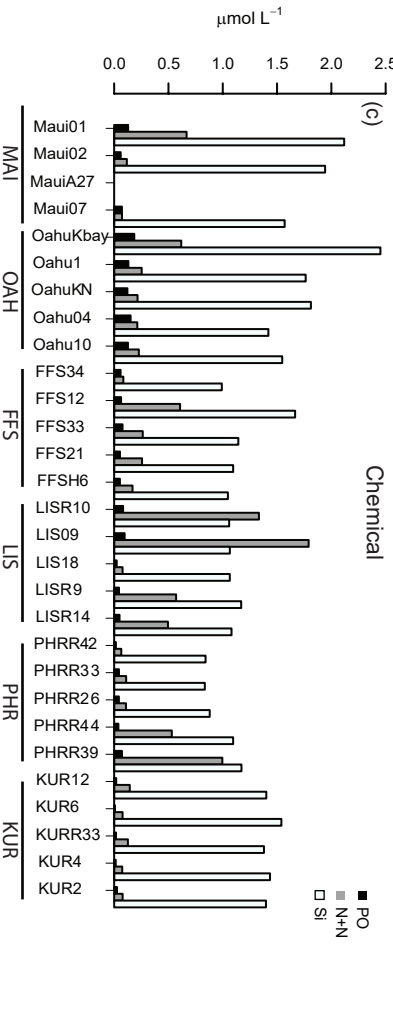
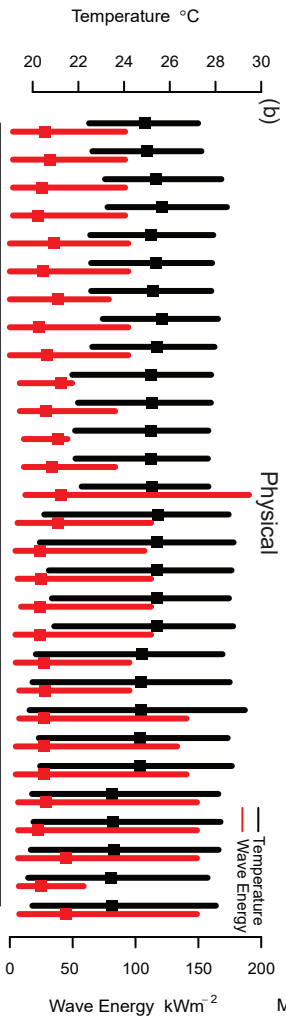
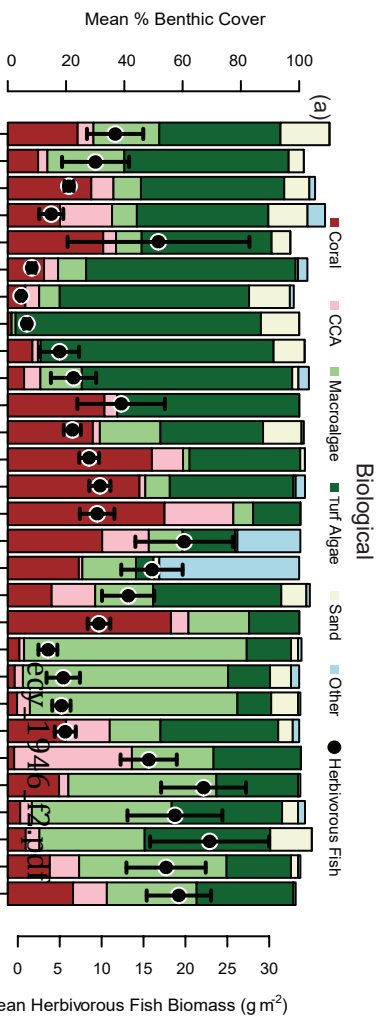
676 are statistically different from each other (pairwise comparisons for site-level data are in Table  
677 S3).

678

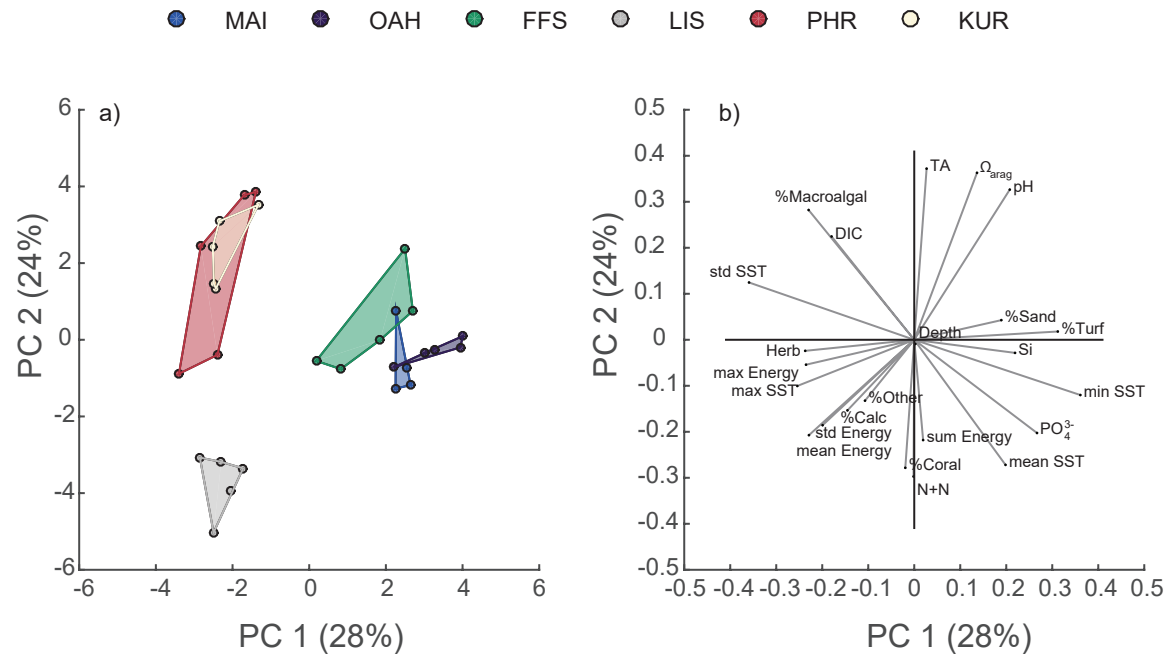
679 **Figure 5: AIC weights (AICw) for environmental parameters versus (a,b) carbonate**  
680 **production, (c,d) bioerosion, and (e,f) net accretion for (a,c,e) the MHI, and (d,b,f) the**  
681 **NWHI.** Each inset shows the top three highest ranking models for each model selection with  
682 bars representing individual environmental models. Signs next to bars represent positive (+) or  
683 negative (-) relationships between environmental drivers and the accretion-erosion rates. Full  
684 model selections are available in Tables S3-S5. X-axes are the AICw values with 1 being the  
685 model with the highest weight. Bar colors represent environmental driver groups.

Author Manuscript





Author Manuscript



# Author Manuscript

This article is protected by copyright. All rights reserved

